Article:
Mukhopadhyay, R., Manjaiah, K.M., Datta, S.C. et al. (2017) Inorganically modified clay minerals: Preparation, characterization, and arsenic adsorption in contaminated water and soil. Applied Clay Science, 147. pp. 1-10. ISSN: 0169-1317

https://doi.org/10.1016/j.clay.2017.07.017

Inorganically modified clay minerals: preparation, characterization, and arsenic adsorption in contaminated water and soil

Raj Mukhopadhyay[a], K. M. Manjaiah[a*], S. C. Datta[a], R. K. Yadav[b], Binoy Sarkar[c,d]

[a]Division of Soil Science and Agricultural Chemistry, ICAR-Indian Agricultural Research Institute, New Delhi 110012, India

[b]Division of Soil and Crop Management, ICAR-Central Soil Salinity Research Institute, Karnal, Haryana 132001, India

[c] Department of Animal and Plant Sciences, The University of Sheffield, Sheffield, S10 2TN, UK

[d]Future Industries Institute, University of South Australia, Mawson Lakes, SA 5095, Australia

*Correspondence to: K. M. Manjaiah, Division of Soil Science and Agricultural Chemistry, ICAR-Indian Agricultural Research Institute, New Delhi 110012, India.

E-mail address: *manjaiah@iari.res.in* (K. M. Manjaiah).

Abstract

The use of modified clay minerals for adsorbing arsenic (As) in contaminated soils is an underexplored area of research. The adsorption behavior of As onto inorganically modified smectite and kaolinite both in aqueous and soil media was studied. X-ray diffraction, infra-red spectroscopy, scanning and transmission electron microscopy studies confirmed successful modification of smectite through Fe-exchange and Ti-pillaring, and kaolinite through phosphate binding. The modified smectites were more efficient than phosphate-bound kaolinite in adsorbing

As both in water and soil systems. Kinetic study revealed that the clay products reached adsorption equilibrium within 3 h, and the data well fitted to the power function and simple Elovich equation ($R^2 > 0.90$). The Freundlich isotherm model best described the As adsorption data ($R^2 > 0.86$) of the modified clay products in both the systems. The Ti-pillared smectite exhibited the highest As adsorption capacity (156.54 $\mu g g^{-1}$) in the aqueous medium, while the Fe-exchanged smectite was the best material in the soil system (115.63 $\mu g g^{-1}$). The partition coefficient (K_d) and adsorption efficiency (%) data also maintained the similar trend. Precipitation of As and binuclear complex formation also took place in the soil system which made the metalloid non-labile as the time passed. The inorganically modified clay products reported here hold a great potential to adsorb As in contaminated groundwater, drinking water as well as soil.

Key words: Arsenic, inorganic modification, smectite, kaolinite, Freundlich isotherm, adsorption

1. Introduction

Arsenic (As) has become a major pollutant in soil and drinking water in many parts of the world. Despite being relatively scarce in the natural environment (0.0005%; 20th abundant element in the continental crust), arsenic is widely distributed over the globe (Gebreyowhannes, 2009). All over the world where arsenic contamination in groundwater and its potentially severe human health effects have been reported, the impact has been the highest in Bangladesh and the Bengal delta basin of West Bengal, India (Chowdhury et al., 2000; Mukhopadhyay et al., 2002). More than 90% of the total groundwater in West Bengal is affected by arsenic contamination (Sanyal and Nasar 2002). The contamination of water occurs due to the dissolution of minerals like arsenopyrites from parent materials, geochemical reactions, biological activities and/or from anthropogenic sources such as the leaching of manmade arsenic compounds from smelting of metal ores, and

wood preservatives (Shevade and Ford, 2004). There are two chemical hypotheses, namely arsenopyrite oxidation hypothesis (Mandal et al., 1996) and ferric oxyhydroxide reduction hypothesis (Bhattacharyya et al., 1997), which explains the widespread arsenic occurrence in the groundwater of Bengal delta basin and Bangladesh. The latter hypothesis proved more consistent according to some literature (Sanyal 1999; Aziz et al., 2016). According to this hypothesis, anoxic condition of the aquifers caused the mobilization of arsenic from arsenic bearing minerals into the groundwater.

Buildup of arsenic in soil due to the use of contaminated groundwater for irrigation has led to a global environmental concern, especially for rice production and food security in South Asia (India and Bangladesh) (Das et al., 2008; Khan et al., 2009). In addition, drinking of arsenic contaminated groundwater is a direct health threat to the people in this region and other parts of the world (Liu et al., 2002; Ng et al., 2003; Das et al., 2011; Sarkar et al., 2016). Consumption of arsenic contaminated drinking water may cause kidney, urinary tract, liver, skin, and rectum cancers in humans (Pontius, 1994). Non-carcinogenic diseases related to arsenic exposure are hypertension, diabetes mellitus, cerebrovascular and cardiovascular systems, and dysfunction of respiratory system (Thomas et al., 2001).

Arsenic is dominantly present in soils in inorganic forms which are a function of redox potential and pH of the medium. Arsenate (As (V)) is the major arsenic species in surface water over the pH range of 5 to 12 (Zeng, 2004). Arsenite (As (III)) is mostly found under reducing conditions, and thus is the most dominant species in groundwater over the pH range of 2 to 9 (Zeng, 2004).

Anion exchange, adsorption, reverse osmosis, coagulation, co-precipitation and solvent extraction are commonly known methods for removing arsenic from aqueous systems (Mohan and Pittman, 2007; Jadhav et al., 2015; Shakoor et al., 2016; Vithange et al., 2017). Various adsorbents

including activated carbon, biochar, agricultural and industrial byproducts, zeolite and clay minerals, metal oxides and hydroxides, nanomaterials and resins were reported to remove arsenic from contaminated water (Mohan and Pittman, 2007; Sharma et al., 2014). However, available technologies for removing arsenic from soils are very limited. Phytoremediation of As from soil could be carried out through plants such as *Pteris vittata* (Mandal et al., 2012; 2017; Fayiga and Saha, 2016; Niazi et al., 2016). Ghosh et al. (2012) used farm yard manure and compost to make chelation of arsenic with humate compounds and immobilize it in soils. While the influence of organic matter on the mobility and bioavailability of arsenic species are ambiguous (Suda and Makino, 2016; Wang et al., 2016), some inorganic amendments such as iron compounds, phosphates, alkaline compounds, gypsum, biosolid, red mud, fly ash and clay minerals were found effective in immobilizing As in soils (Lombi et al., 2004; Kumpiene et al., 2008; Miretzky and Cirelli, 2010; Lee et al., 2011; Lim et al., 2016). However, many of these materials are expensive and still do not have standard protocol of practical soil application.

Due to their low cost, worldwide distribution and superior physico-chemical properties (e.g., high specific surface area, ion-exchange capacity, mechanical stability and lamellar structure), clay minerals (with or without modification) have also found widespread research attention in the remediation of metals and metalloids in water and soil (Sarkar et al., 2012; 2013; Sun et al., 2013; Perelomov et al., 2016; Kumararaja et al., 2017). In addition, such materials are ideal for one-time use requiring no regeneration.

Clay minerals modified with different inorganic ions like Fe, Al, Ti, organic acids, mineral acids, polymers, surfactants and nanoparticles were found promising for As remediation in contaminated water (Li et al., 2007; Boddu et al., 2008; Doušová et al., 2009; Akpomie and Dawodu 2016; Sarkar et al., 2016). Ti-pillared smectite was considered in the present investigation due to its high

adsorption affinity towards arsenic in aqueous system as it forms a polyhydroxy stable complexation with arsenic. Similarly the Fe-exchanged smectite forms stable iron-arsenate which enhanced arsenic adsorption efficiency in aqueous system. However, use of these modified clay minerals for the adsorption of As in contaminated soils is still an underexplored area of research. There is an urgent need to develop cost-effective methods for the removal/immobilization of As in contaminated soils. Therefore, the present study aimed to prepare and characterize three different inorganically modified clay minerals (Fe-exchanged and Ti-pillared smectite, and phosphate-bound kaolinite), and compare their As adsorption behavior in contaminated water and soil.

2. Materials and Methods

2.1 Chemicals and clay minerals

Potassium dihydrogen phosphate (KH_2PO_4), iron sulphate heptahydrate ($FeSO_4.\ 7H_2O$), calcium chloride dihydrate ($CaCl_2.2H_2O$) and other chemicals were of analytical grade and purchased from Merck Millipore, Mumbai, India. Sodium arsenate heptahydrate ($Na_2HAsO_4.7H_2O$), and titanium chloride ($TiCl_4$) were purchased from Sigma-Aldrich Chemicals Pvt. Ltd., New Delhi, India. The As stock solution (1000 mgL^{-1}) was prepared using $Na_2HAsO_4.7H_2O$ in 0.01 *M* $CaCl_2$ in double distilled water. The working solutions of As were freshly prepared by diluting the stock solution in 0.01 *M* $CaCl_2$ solution. 0.1 *N* HNO_3 and 0.1 *N* NaOH were used to adjust the pH of As solutions as necessary.

The smectite and kaolinite samples in the form of bentonite and kaolin were purchased respectively from S D Fine-Chem Limited, Mumbai, India and Molychem, Mumbai, India. The clay samples contained 88% smectite (kaolinite and quartz as impurities) and 86% kaolinite (Fe-oxides and

quartz as impurities), respectively, as the main mineral composition. The average particle size of unmodified, Fe-exchanged and Ti-pillared smectite was 158.10, 169.30 and 174.60 nm, respectively, while this values was 189.40 and 171.70 nm, respectively, for unmodified and phosphate-bound kaolinite. In order to reduce the cost of production, the raw materials were used as received without any purification.

2.2 Soil sample

Arsenic contaminated soil sample was collected (0-15 cm depth, order: Inceptisol) from Mitrapur, West Bengal, India (22.9981° N and 88.6121° E). The collected soil sample was air dried under shade and ground with mortar and pestle. The ground sample was passed through 2-mm sieve for further analysis purposes. The As content and other physico-chemical characteristics of the soil are given in Table 1.

2.3 Preparation of inorganically modified clay minerals

2.3.1 Preparation of iron-exchanged smectite

The smectite sample was treated with 0.1 *M* $FeSO_4$ solution in double distilled water (Te et al., 2015). In brief, 20 g of dried smectite was mixed with 200 mL of 0.1 *M* $FeSO_4$ in a 250 mL conical flask and stirred for 24 h in a mechanical shaker with a speed of 200 rpm at room temperature. The solid smectite was separated using centrifugation technique (4000 rpm for 5 min) and dried at 105°C for 24 h. The dried smectite sample was further heated to 350°C in a muffle furnace for 3 h and cooled to room temperature. Furthermore, the sample was washed with double distilled water until no reddish colour appeared upon addition of 1:10 phenanthroline (negative test for Fe) and dried at 60°C for overnight in a hot air oven.

139

140 *2.3.2 Preparation of Ti- pillared smectite*

141 At first, Na-smectite was prepared by adding 0.1 *M* NaOH drop by drop to a smectite suspension
142 (10% w/v) under continuous stirring in a magnetic stirrer for 16 h. The saturated particles were
143 separated through centrifugation (5000 rpm for 10 min) and washed with double distilled water
144 until it became chloride free (no white precipitation upon the addition of a drop of 0.1 *N* $AgNO_3$
145 solution). Then Na-smectite was dried at 80°C for 4 h for further use. Ti-pillaring of Na-smectite
146 followed the procedure of hydrolysis of $TiCl_4$ in reaction with HCl as described by Na et al. (2010).
147 In short, 100 mL of $TiCl_4$ was dissolved in 200 mL of 3 *M* HCl solution under vigorous stirring
148 for 2 h. The resultant solution was mixed with a 0.5 *M* HCl solution (1:2.5 ratio), and the pillaring
149 agent was obtained. Na-smectite (10 g) was slowly added to 490 mL of double distilled water
150 under stirring at 2000 rpm for 1 h. Then the mixture was aged for 12 h at 25°C. The pillaring agent
151 was then added into this mixture over a period of 1 h under vigorous stirring at about 3000 rpm.
152 Afterwards, the mixture was transferred to a bottle and treated in a water bath at 80°C for 6 h. The
153 product obtained was then filtered and washed with distilled water, dried, ground to powder.

154

155 *2.3.3 Preparation of phosphate-bound kaolinite*

156 The kaolinite sample was modified with KH_2PO_4 solution following the procedure of Amer et al.
157 (2010). Kaolinite (100 g) was equilibrated with 1 L of 200 mgL^{-1} KH_2PO_4 in a rotary orbital shaker
158 at 150 rpm for 24 h. The sample was then washed several times with double distilled water to
159 remove excess phosphate from the mineral surface. Phosphate in the washout solution was found
160 negative, and the clay sample was dried in the oven at 105°C for 24 h.

161

2.4 Characterization

The cation exchange capacity (CEC) of the clay minerals (modified and unmodified) was determined by $CaCl_2$-$MgCl_2$ method (Alexiades and Jackson, 1965) and specific surface area was calculated using EGME (ethylene glycol monoethyl ether) adsorption method (Heilman et al., 1965).

X-ray diffraction analyses of the powdered samples were performed using a Philips PW1710 X-ray diffractometer with a monochromatic Cu-Kα (λ = 1.5418 Å) source operating at 40 kV and 20 mA. The diffraction pattern recorded from 4° to 30° with a scan rate of 1.5° 2θ min^{-1}.

Fourier transform infra-red spectroscopy (FTIR) of the samples was carried out in the form of KBr pellets using Bruker ALPHA, FTIR/ATR system (typically 64 scans, resolution 4 cm^{-1}), and samples were scanned in 4,000-600 cm^{-1} region. Scanning electron microscopy (SEM) images of the clay products were taken using a VEGA3 LM scanning electron microscope (Tescan Orsay Holding Instrument, Czech Republic) equipped with backscattered electron (BSE) and secondary electron (SE) detectors.

Transmission electron microscopy (TEM) images of all the modified clay products were taken using a JEOL TEM model JEM-1101 (JEOL Ltd., Japan).

2.5 Adsorption studies

2.5.1 Adsorption kinetics

The kinetics of As adsorption was performed at room temperature (25±1°C) and pH 6.2 (maintained with 0.1 *N* NaOH and 0.1 *N* HNO_3) with an As (arsenate) concentration of 50 μg mL^{-1}. Each type of unmodified and modified clay mineral (0.5 g) (solid: solution=1:20) was equilibrated in triplicate with the As solution in plastic centrifuge tubes (50 mL) on an end over

end shaker (225 rpm). Two blanks (without adsorbent and water without As) were taken as controls. The samples were equilibrated for different time intervals (20, 40, 60, 80, 100, 120, 140, 160 and 180 min). After equilibration, the clay samples were centrifuged at 10,000 rpm for 10 min using a REMI-24 research centrifuge (REMI, Mumbai, India). The supernatant was immediately filtered through 0.45-µm membrane filter. Final volume of the filtrate was made up using 2% HNO_3 to avoid any damage to the interface on the instrument. The concentration of As in the filtrate was analyzed against a standard As solution provided by the National Institute of Standards and Technology (NIST) (purchased from Merck Millipore, Mumbai, India) using an inductively coupled plasma mass spectrophotometer (ICP-MS) (Perkin Elmer NexION 300X, USA). The amount of As adsorbed at time t (q_t) (µg g^{-1}) was calculated from the mass balance relationship using Eq. 1:

$$qt = \frac{(C0 - Ct)\ v}{m} \quad \text{(Eq. 1)}$$

where, C_0 and C_t are the concentrations of As (µg mL^{-1}) at time zero and t, respectively; v is the volume of As solution (mL); and m is the mass (g) of adsorbent. At equilibration, q_t was called as the equilibrium adsorption and C_t was known as the equilibrium concentration.

2.5.2 Adsorption isotherm in aqueous system

Various clay adsorbents (1 g) were weighed and taken in plastic centrifuge tubes (50 mL). Arsenic solutions (20 mL) of various concentrations (2.5 to 50 µg mL^{-1} in 0.01 *M* $CaCl_2$) were then added into the tubes. The suspensions were equilibrated for 24 h on an end over end shaker (225 rpm) to ensure the equilibrium. All the experiments were conducted in triplicate at room temperature (25 ± 1°C) and pH 6.2 (maintained with 0.1 *N* HNO_3 and 0.1 *N* NaOH). After equilibration, the supernatants were separated and analyzed for As concentrations by ICP-MS as described earlier.

Blank tests under the same conditions revealed no As adsorption on the tube wall during the reaction period. The amount of As adsorbed was calculated using Eq. 1, and the As adsorption efficiency (%) was calculated using Eq. 2:

$$\text{Adsorption efficiency (\%)} = \frac{(C0-Ce)}{C0} \times 100 \quad \text{(Eq. 2)}$$

where, C_0 is the As concentration (μg mL^{-1}) at time zero; C_e is the equilibrium As concentration (μg mL^{-1}) at time t.

2.5.3 Adsorption isotherm in soil system

The As contaminated soil (1.5 g) was amended with each type of clay products at 0.25% (w/w) application rate in plastic centrifuge tubes. Then, 30 mL aqueous solutions of As (2.5 to 50 μg mL^{-1} in 0.01 *M* $CaCl_2$) were added to the soil. Further experimental procedures and conditions were maintained similar to those described earlier. All experiments were conducted in triplicate. Two blank tests were conducted with soil (absence of clay products) and without soil (absence of both soil and clay product). No As was adsorbed on the wall of the tubes. The amount of As adsorbed by the clay products was calculated by subtracting the amount adsorbed by the soil (absence of clays) from the amount adsorbed by the soil amended with the clay products using the mass balance relationship (Eq. 1). Similarly, the As adsorption efficiency (%) of different clay products in the soil system was calculated using Eq. 2.

2.5.4 Partition coefficient (K_d)

The K_d value (partition coefficient) of As adsorption on different modified clay minerals in the aqueous and soil system was calculated using Eq. 3:

$$Kd = qe/Ce \quad \text{(Eq. 3)}$$

where, K_d (mL g^{-1}) is the partition coefficient of As adsorption; q_e is the amount of As adsorbed per unit mass of adsorbent at equilibrium (μg g^{-1}); C_e is the equilibrium As concentration (μg mL^{-1}).

2.6 Statistical analyses

The kinetic and isotherm data of As adsorption were fitted to model equations (power function and simple Elovich model for adsorption kinetic study, and Freundlich model for adsorption isotherm study) by nonlinear regression using least squares method. The correlation coefficients (R^2) obtained from the regressions analyses were used to evaluate the applicability of the model equations.

3. Results and Discussion

3.1 Characterization of clay products

3.1.1 General properties

Selected physico-chemical properties of the unmodified and modified clay minerals are given in Table 2. The raw smectite was alkaline in nature (pH 8.20), while the kaolinite was neutral in reaction (pH 6.75). After reactions of smectite with $FeSO_4$ and $TiCl_4$, the products' pH values decreased drastically to 3.93 and 5.95, respectively. This was because of saturation of the clay mineral with cations (Fe^{2+} and Ti^{4+}) and also hydrolysis in the case of Ti-pillaring in the presence of HCl. The pH of the kaolinite changed only slightly (pH 6.50) following the modification with phosphate. The specific surface area (SSA) of the unmodified smectite was 202.69 $m^2 g^{-1}$, whereas it had increased up to 2-folds in Fe-exchanged smectite and Ti-pillared products (485.62 and 437.06 $m^2 g^{-1}$, respectively). The SSA of kaolinite also increased by five times from 18.40 to 89.08

254 m^2 g^{-1} after the modification with phosphate (Adebowale et al., 2006). The SSA increase in the
255 clay products was likely due to the removal of impurities from the clay minerals (Rusmin et al.,
256 2016). Additionally, the replacement of exchangeable cations, particularly with Fe^{2+} and Ti^{4+},
257 might have exposed the clay edges and increased the SSA (Akpomie and Dawodu, 2016). The
258 cation exchange capacity (CEC) of the unmodified smectite and kaolinite was 118.50 and 22.25
259 cmol (p^+) kg^{-1}, respectively, whereas the value was 115.75, 105.75 and 40.50 cmol (p^+) kg^{-1} for
260 Fe-exchanged smectite, Ti-pillared smectite and phosphate-bound kaolinite, respectively. The
261 CEC of smectite decreased after the exchange and pillaring reactions because the guest cations
262 and polyhydroxy titanium might have blocked the adsorption sites (Karamanis et al., 1997).
263 However, CEC of kaolinite was increased due to ligand adsorption of phosphate on to the clay
264 mineral surface (Ioannou and Dimirkou, 1997).
265
266 *3.1.2. X-ray diffraction (XRD)*
267 The XRD patterns of the unmodified and modified clay products are given in Fig. 1. The d(001)
268 value (basal spacing) was calculated from the corresponding first order reflection of the 001 plane.
269 A successful modification of the interlayer environment of the smectite was confirmed by the
270 deviation in the 2θ angle of the corresponding 001 reflection. The d(001) value of the unmodified
271 smectite was 14.24 Å (Fig. 1; Table 2) which was comparable to the d (001) value of a typical
272 montmorillonite. Both the Fe-exchanged and Ti-pillaring modifications resulted in an increase of
273 the d(001) value (interlayer expansion) (Fig. 1). The increase in d(001) value of Fe-exchanged and
274 Ti-pillared smectite was 2.11 and 2.73 Å, respectively (Table 2), which was in alignment with
275 previous reports (Karamanis et al., 1997; El Miz et al., 2014). Conversely, the d(001) values of the

kaolinite and phosphate-bound kaolinite were 7.25 and 7.13 Å, respectively (Fig. 1), indicating that phosphate might have attached only on broken edges of the kaolinite (Bidwell et al., 1970).

3.1.3 Functional group analysis

The FTIR bands at 3642 and 3452 cm^{-1} (Fig. 2) in the spectra of unmodified smectite were attributed to –OH bending mode of the adsorbed water (Farmer, 1974). Two other bands at 2435 and 1654 cm^{-1} were ascribed to the basic layer silicate structure of smectite (Madejova and Komadel, 2001). The bands at 1037 and 959 cm^{-1} were due to the stretching vibration of Si-O-Si groups and bending vibration of Al-O(OH)-Al groups, respectively (Madejova and Komadel, 2001). In the FTIR spectrum of Ti-pillared smectite (Fig. 2), the band at 3642 cm^{-1} shifted to 3696 cm^{-1}, and the band due to vibration of water molecules in interlayer shifted to 3397 cm^{-1} (Zhang et al., 2008). Similarly, in the spectrum of Fe-exchanged smectite (Fig. 2), the band at 3642 shifted to 3690 cm^{-1}, and the water molecules band moved to 3394 cm^{-1}. The shifting of bands from 3696 cm^{-1} to the region of 3390 cm^{-1} in both of the modified clay products suggested the H-bond formation (Zhang et al., 2008). The presence of bands around 2419 cm^{-1}, 2412 cm^{-1} and 1698 cm^{-1} in both spectra of the modified clay products proved that their layer silicate structures were preserved. The band around 1037 cm^{-1} indicated Si-O-Si bonding in both the modified smectites. The band at 962 cm^{-1} in the spectrum of Fe-exchanged smectite confirmed the presence of Al-O-Al bonding which was minimized in the case of Ti-pillared smectite. The presence of new bands at 621cm^{-1} in the spectrum of Ti-pillared smectite and at 634 cm^{-1} in Fe-exchanged smectite might be due to the formation of Si-O-Ti and Si-O-Fe bonds, respectively (Zhang et al., 2008). In both unmodified and modified kaolinites, the appearance of the bands around 3690 and 3680 cm^{-1}, which were attributed to the stretching vibration of inner surface hydroxyl groups (Fig. 2)

299 (Unuabonah et al., 2008; Amer et al., 2010). The band at 3551 cm^{-1} was attributed to the OH
300 stretching vibration of inner hydroxyl group (Unuabonah et al., 2007). The band at 3551 cm^{-1} in
301 the spectrum of kaolinite was splited to 3503 and 3464 cm^{-1} in the phosphate-bound product (Fig.
302 2). The bands at 2414 and 1717 cm^{-1} in the unmodified kaolinite attributed to the typical layer
303 silicate structures and were found unchanged after the phosphate modification. The bands at 1035,
304 916 and 697 cm^{-1} in kaolinite were ascribed to Si-O-Si bond, Al-O(OH)-Al bond and Al-O bond,
305 respectively (Unuaboanh et al., 2008). Only the band for Si-O-Si bond shifted from 1035 to 1027
306 cm^{-1} after phosphate modification (Amer et al., 2010).
307
308 *3.1.4 SEM characterization*
309 The surface of the unmodified smectite was smooth and crystalline in structure (Fig. 3). However,
310 after modification, the Ti-pillared and Fe-exchanged smectite became swollen, fluffy and slightly
311 clustered (Akpomie and Dawodu, 2016). Swollenness and fluffiness occurred likely due to
312 increase in d(001) values of the clay mineral following modification. These changes were very
313 clear in Ti-pillared and Fe-exchanged smectite (Fig. 3). The SEM image of the unmodified
314 kaolinite was very tiny and thin plate like structural surface (Fig. 3). The kaolinite also became
315 little bit aggregated in its surface morphology after the phosphate modification (Fig. 3)
316 (Unuabonah et al., 2008).
317
318 *3.1.5. TEM characterization*
319 The approximate shape and size of the clay products were determined through TEM images (Fig.
320 4). The shape of smectite particle appeared as a clear crystalline structure with an approximate
321 length 41.82 nm (in one dimension) (Fig. 4). But after modification, the shapes of Ti-pillared and

Fe-exchanged smectite (Fig. 4) particles became cloudy, fluffy, swollen and slightly clustered due to increase in basal spacing (Seki and Yurdakoc, 2007), as was also observed in SEM images. The approximate one dimensional length of Ti-pillared and Fe-exchanged smectite particles was 47.50 and 44.87 nm, respectively. The unmodified kaolinite particles appeared as a clear hexagonal, thin plate like structure (Fig. 4) with approximate length of 275.78 nm (Ma and Eggleton, 1999). The shape of phosphate-bound kaolinite (Fig. 4) did not change significantly, but remained clustered. The approximate length of phosphate-bound kaolinite particle was 150.59 nm. This huge variation in the length of kaolinite minerals before and after the phosphate modification might be due to their irregular shaped particle distribution (Hassan and Abdu, 2014). Therefore, the TEM images substantiated the SEM surface morphology results discussed earlier.

3.2. Arsenic adsorption kinetics

The initial adsorption of As on Ti-pillared smectite was slightly lesser than Fe-exchanged and unmodified smectite (Fig. 5). The amount of As adsorbed were 448.0, 536.0 and 479.2 $\mu g g^{-1}$ by Ti-pillared, Fe-exchanged and unmodified smectite at initial 20 min of adsorption (Fig. 5), which suggested that Fe-exchanged smectite required less contact time to remove As from aqueous system than the other two clay products. The exchanged iron (Fe) in the interlayer of smectite probably formed iron hydroxides and oxides through oxidation and hydration processes during reaction with water in the interlayer and the oxygen atoms at the end of each sheet of the clay mineral (Stucki et al., 2002). The faster adsorption mechanism was in agreement with previous reports using crystalline hydrous ferric oxide (Manna et al., 2003). Moreover, Fe had greater affinity to adsorb As species than Ti (Lenoble et al., 2002). The Ti-pillared smectite started rapid adsorption after a slow start. But from 40 minutes onwards, the Fe-exchanged smectite exhibited

more or less uniform adsorption rate and the trend continued throughout the rest of the reaction period. In aqueous medium, Ti-pillared smectite adsorbed As by chemisorption mechanism (Lenoble et al., 2002; Na et al., 2010). The chemisorption reaction mechanism of arsenate adsorption onto Ti-pillared smectite in aqueous system is as follow:

$$M(OH)_{(s)} + H^{+} \leftrightarrow M(OH_2)^{+}_{(s)} \quad \text{(Eq. 4)}$$

$$M(OH)_{(s)} + H_2AsO_4^{-}{}_{(aq)} \leftrightarrow MHAsO_4^{-}{}_{(s)} + H_2O_{(aq)} \quad \text{(Eq. 5)}$$

$$M(OH)_{(s)} + H_2AsO_4^{-}{}_{(aq)} \leftrightarrow MHAsO_4^{2-}{}_{(s)} + H^{+}_{(aq)} + H_2O_{(aq)} \quad \text{(Eq. 6)}$$

$$M(OH_2)^{+}_{(s)} + H_2AsO_4^{-}{}_{(aq)} \leftrightarrow M(OH_2)_{(s)} - H_2AsO_4^{-}{}_{(s)} \quad \text{(Eq. 7)}$$

where, $M(OH)_{(s)}$ represents a hydroxy group of the Ti-pillared smectite; $H^{+}_{(aq)}$ is the solution pH; $MHAsO_{4(s)}$ and $MAsO_{4(s)}$ the inner sphere complex, and $M(OH_2^{+}) - H_2AsO_{4(s)}$ the outer sphere complex of arsenate.

After 3 h of reaction, Fe-exchanged smectite indicated a higher As adsorption (582.8 $\mu g g^{-1}$) than unmodified (530.8 $\mu g g^{-1}$) and Ti-pillared smectite (490.0 $\mu g g^{-1}$). The arsenate species ($H_2AsO_4^{-}$) in aqueous phase is mostly dominant in between pH 2.2 to 6.98. Surface of the Fe-exchanged smectite became more positively charged due to acidic nature of Fe-exchanged smectite and the medium, which formed stable iron arsenate (Te et al., 2015). This might be a probable mechanism of As adsorption by Fe-exchanged smectite. On the other hand, phosphate-bound kaolinite also adsorbed a lesser amount of As (454.0 $\mu g g^{-1}$) than unmodified kaolinite (467.6 $\mu g g^{-1}$) initially at 20 min of reaction (Fig. 5), which indicated kaolinite's greater initial As removal capacity than the modified product. It was likely due to the presence of some positive surface charges on broken edges of the kaolinite as a function of mild acidic reaction (pH 6.2). It was reported that As adsorption was regulated by its type of solution species, especially As (V) and surface charge (Xu et al., 1988; Manning and Goldberg, 1996). But from 60 min onwards, unmodified kaolinite started

adsorbing considerably less amount than the phosphate-bound kaolinite. At equilibration, phosphate-bound kaolinite adsorbed (502.2 $\mu g g^{-1}$) more than the unmodified kaolinite (495.0 $\mu g g^{-1}$). The results demonstrated that all these clay minerals and their products increased As removal at equilibrium (3 h). A similar inference was drawn by several researchers (Zeng, 2004; Mohapatra et al., 2007; Na et al., 2010) who used different types of smectite and kaolinite. However, among all the clay minerals, Fe-exchanged smectite exhibited the maximum As adsorption (582.8 $\mu g g^{-1}$) and highest As removal capacity.

Two adsorption kinetic models (power function and simple Elovich) were used to fit the kinetic data by nonlinear regression (Sparks, 1989). These models are expressed respectively by Eq. 8 and 9:

Power function equation: $q = a\, t^{b}$ (Eq. 8)

where, q = adsorbed As ($\mu g g^{-1}$) at time t (min); a and b are the constants; b is positive and less than 1.

Elovich equation: $q = a + b \ln t$ (Eq. 9)

where, q = adsorbed As ($\mu g g^{-1}$) at time t (min); a is intercept and b is the slope. The simple Elovich parameters were estimated without using the origin (q = 0, t = 0).

On the basis of R^2 values (>0.90), the kinetics of As adsorption onto different clay minerals could be described by both the model equations (Table 3). A similar kind of inference about well fitted kinetics model of As adsorption was drawn by Zeng (2004) using a Fe (III)-Si binary oxide adsorbent. The higher value of 'a' in the power function equation suggested the higher adsorbed amount of adsorbate with time. Similarly, in simple Elovich equation, high value of slope 'b' and intercept 'a' implied higher adsorption rate with time (Sparks, 1989).

391 *3.3. Adsorption isotherm study in aqueous system*

392 The unmodified smectite was a poor adsorbent of As in aqueous system because of its low
393 adsorption efficiency (48.56%) (Table 4). The Fe-exchanged and Ti-pillared smectites gave 73.64
394 and 78.82% sorption efficiency, respectively. The adsorption efficiencies were 66.07 and 79.05%
395 in unmodified kaolinite and phosphate-bound kaolinite, respectively. High adsorption efficiency
396 of modified smectite can be explained by high specific surface area and more availability of
397 exchangeable sites. Earlier, Grygar et al. (2007) reported that As adsorption was enhanced due to
398 the presence of high amount of Fe in Fe-exchanged smectite. Ti-pillared smectite gave the highest
399 adsorption efficiency among all the smectites. Owing to the expansion of the interlayer after Ti-
400 pillaring. The polyhydroxy titanium cations led to the generation of many active OH^- ions. Later
401 on, As species formed complexation with OH^- ions of smectite in the aqueous system (Na et al.,
402 2010). The adsorption efficiency of unmodified kaolinite was higher than unmodified smectite.
403 The edges of kaolinite might have provided some positive surface charges due to the presence of
404 mild acidic aqueous medium (pH 6.2) and As could form an aqua complexation (Mohapatra et al.,
405 2007). The phosphate-bound kaolinite accounted for higher adsorption efficiency likely due to its
406 higher surface area and the ligand exchange between phosphate and solution As species. Like the
407 adsorption efficiency, average partition coefficient [K_d (mLg^{-1})] followed a similar trend. The Ti-
408 pillared smectite exhibited the maximum K_d value (175.77) followed by Fe-exchanged smectite
409 (121.89), phosphate-bound kaolinite (109.46), unmodified kaolinite (85.20) and unmodified
410 smectite (67.30) (Table 4). Ramesh et al. (2007) reported that the K_d value increased for As
411 adsorption because of the increased surface area and availability of more exchangeable sites in
412 polymeric Fe-modified montmorillonite. Therefore, variations in K_d values of different modified
413 clay products might be supported by the reasons explained for the adsorption efficiencies. Simply,

414 higher the sorption efficiency, higher is the partition coefficient. However, in general, with the
415 increasing equilibrium concentration of As, the adsorption amount decreased onto the clay
416 products in the aqueous system.
417 Freundlich adsorption isotherm has more flexibility. Any changes in adsorption behavior can be
418 best described by Freundlich isotherm. Data for As adsorption onto different clay minerals in
419 aqueous system (Fig. 6) was fitted to the Freundlich isotherm model only (Eq. 10) due to surface
420 heterogeneity of the modified clays and high significant coefficient of determination (R^2).

421 $$q = K\,C^{1/n} \qquad \text{(Eq. 10)}$$

422 where, q is the amount of adsorbed As on different clay minerals at equilibrium ($\mu g g^{-1}$), and C is
423 the As equilibrium concentration in solution ($\mu g\ mL^{-1}$), K and (1/n) are the Freundlich constants.
424 K represents the adsorption of As at equilibrium concentrations, and (1/n) indicates the degree to
425 which adsorption is a function of As concentration (Table 5).
426 The 1/n values signify the degree of the intensity of adsorption. The 1/n values for As adsorption
427 on the modified clay minerals were less than unity indicating L-type isotherms (Giles et al., 1960).
428 L-type isotherms are characterized by the decrease in the adsorption at higher aqueous
429 concentrations of the solute. This suggests a greater competition for adsorption sites which become
430 limited as solute concentration in solution increases.
431 To obtain a meaningful comparison of their K values, the 1/n values for all modified clay minerals
432 should nearly be equivalent. The K ($\mu g g^{-1}$) value or As adsorption capacity was the maximum in
433 Ti-pillared smectite (156.54), followed by Fe-exchanged smectite (127.63), phosphate-bound
434 kaolinite (124.43), unmodified kaolinite (93.82) and unmodified smectite (66.03). The higher K
435 value might be explained by the respective K_d values. The higher partition coefficient (K_d)
436 suggested higher As adsorption capacity (K) by the modified clay products. The other reason might

be the surface complexation which is one of the stable bond formations that occurred in the case of Ti-pillared smectite. The R^2 obtained for Freundlich model fitting were more than 0.90 for all modified clays except the unmodified smectite and kaolinite (Table 5). Arsenate and arsenite adsorption on iron oxide-coated sand and ferrihydrite was also best described earlier by the Freundlich isotherm model (Thirunavukkarasu et al., 2001). The Freundlich isotherm model fitted the experimental data very well due to the heterogeneous distribution of active sites on the modified clay mineral surfaces. The 1/n values of all the clay minerals were less than 1 (Table 5), which suggested that the adsorption process was favorable (Treybal, 1980). Similar results of Freundlich model fitting and 1/n values less than unity for the adsorption of As (V), As (III) and organic As species on polymeric Al/Fe-modified montmorillonite was reported by Ramesh et al. (2007). Among all the smectites, Ti-pillared smectite adsorbed the maximum amount of As, followed by Fe-exchanged and unmodified smectite (Fig. 6). The phosphate-bound kaolinite adsorbed more As than unmodified kaolinite (Fig. 6). The reason might be that As has more spatial compatibility with the adsorption sites of modified clay minerals because of their high surface area. Therefore, the highest As adsorption capacity (K) onto the modified clay minerals in aqueous system maintained the order: Ti-pillared smectite > Fe-exchanged smectite > phosphate-bound kaolinite > unmodified kaolinite > unmodified smectite.

3.4 Adsorption isotherm study in soil system

Very few studies so far focused on the adsorption of As by modified clay minerals in contaminated soils (Sarkar et al., 2012). The adsorption behavior of different modified clay minerals in the soil system was slightly different from that of the aqueous system (Table 4). The adsorption efficiencies were in the order: Fe-exchanged smectite > Ti-pillared smectite > phosphate-bound

460 kaolinite > unmodified kaolinite > unmodified smectite (Table 4). The maximum adsorption
461 efficiency of the Fe-exchanged smectite could be explained by higher surface area and higher
462 positive charge of Fe-exchanged smectites due to reduction in pH (Table 2). Similarly, the
463 increased surface area and ligand exchange reaction imparted greater adsorption efficiency by
464 phosphate-bound kaolinite than the unmodified kaolinite. Phosphate and arsenate ions could
465 compete non-specifically for ligand exchange and complexation sites on kaolinite when present
466 simultaneously in the soil system (Goldberg, 2002). But following modification with phosphate,
467 the kaolinite adsorbed more As than the unmodified counterpart. Earlier, Violante and Pinga
468 (2002) also reported a higher affinity of kaolinite to adsorb arsenate than phosphate. The
469 adsorption mechanism of Ti-pillared smectite would be the same as discussed in the aqueous
470 system. Partition coefficient [K_d (mLg^{-1})] values also followed the same trend of adsorption
471 efficiencies (Table 4). The Fe-exchanged smectite had the maximum K_d (100.13) value (Table 4).
472 However, adsorption efficiencies (except in unmodified smectite) and K_d values for all clay
473 products became lower in the soil system than the aqueous system because the former system was
474 more heterogeneous than the latter. In soil system several factors (e.g., clay type and content,
475 amorphous Fe content, total Fe content, soil pH and organic carbon) (Table 1) (Rivaz-Perez et al.,
476 2015) along with competitive ions might have influenced arsenic adsorption behavior on modified
477 clay minerals.
478 Arsenic adsorption data in the soil system were also fitted to the Freundlich equation (Eq. 10)
479 having $R^2 > 0.85$. Like the aqueous system, here also the 1/n values were less than unity (Table 5).
480 The Freundlich coefficient K ($\mu g g^{-1}$) was the highest in Fe-exchanged smectite (115.63) followed
481 by other clay products and maintained the same trends of adsorption efficiency and partition
482 coefficient (K_d) (Table 5). The pH of contaminated soil was 6.49, which was almost equal to the

483 pH value (6.2) maintained in the solid-solution interaction experiment. Mohapatra et al. (2007)
484 reported that montmorillonite and kaolinite adsorbed the maximum amount of arsenate at pH 6.0
485 and 5.0, respectively. As a result, the modified kaolinite accounted for a lesser K value for As
486 adsorption than the modified smectite.
487 Fig. 7 depicted some irregular or discontinuous adsorption trend followed in the soil system. With
488 the increase in solute concentration, there were breaks and reverse turns in the adsorption curves
489 for both smectite and kaolinites. The Fe-exchanged smectite and unmodified kaolinite exhibited a
490 more continuous increasing trend of adsorption than the other clay products (Fig. 7). The
491 deviations were greater at relatively higher equilibrium concentration of As. Ti-pillared smectite,
492 unmodified smectite and phosphate-bound kaolinite started showing the reverse breaks after 14.3,
493 22.74 and 12.11 $\mu g\ mL^{-1}$ equilibrium concentrations, respectively. This discontinuous trend of
494 solute concentration could be explained by the formation of binuclear As complexes and As
495 precipitation in the soil system (Datta 2002). In a similar fashion, phosphorus solution
496 concentration sharply decreased after attaining a maximum value due to the precipitation of
497 phosphorus in soil (Datta 2002). The non-labile P formation took place due to binuclear complex
498 formation and precipitation (Datta 2002). The precipitated phosphorus became crystallized and
499 non-labile with time (Datta 2002). Arsenic is also analogous to phosphorus (Marschner, 1995),
500 and probably followed the same mechanism in the soil system. Therefore, binuclear complexes
501 and precipitation might have taken place on the surfaces of these modified clay products in soil as
502 a function of soil constituents and competitive anions. Thus, precipitation or binuclear complex
503 formation of As by these modified clay products was quite effective to immobilize As from labile
504 form to non-labile form in the soil.
505

4. Conclusions

Modifications of smectite and kaolinite through Fe-exchange, Ti-pillaring and phosphate binding were confirmed by XRD, FTIR, SEM and TEM characterization techniques. The smectite products (Fe-exchanged and Ti-pillared) were more efficient in As adsorption than phosphate-bound kaolinite in both soil and aqueous systems. While the Ti-pillared smectite was the most suitable product for As adsorption in the aqueous system due to surface complex formation, the Fe-exchanged smectite showed the best effectiveness in the soil system because of its high surface area (485.62 m^2 g^{-1}) and higher affinity to As. The phosphate-bound kaolinite adsorbed As to a greater extent than unmodified kaolinite through ligand exchange mechanism in both the systems. One of the most important properties exhibited by some of the clay minerals was As precipitation and/or binuclear complex formation in the soil system. This made As non-labile in soil with time passed, which was most desirable and effective in remediating the metalloid. Thus, the application of these modified clay products hold a great potential to immobilize As not only in contaminated groundwater and drinking water, but also in contaminated soil.

Acknowledgments

The first author is thankful to Post Graduate School, Indian Agricultural Research Institute (IARI), New Delhi, India for providing IARI-merit Fellowship. All authors sincerely acknowledge the facilities provided by Dr. Gautam Chawla, Division of Nematology, and Dr. Rajendra Prasad Pant, Division of Plant Pathology, IARI, New Delhi, for the SEM and TEM characterization, respectively. The authors are also thankful to the Head, Division of Soil Science and Agricultural Chemistry, IARI, New Delhi for providing facilities during all the experiments.

529 **References**

530 Adebowale, K.O.; Unuabonah, E.I.; Olu-Owolabi, B.I., 2006. The effect of some operating
531 variables in the adsorption of lead and cadmium ions on kaolinite clay. J. Hazard. Mater.
532 134, 130-139.

533 Akpomie, K. G.; Dawodu, F.A., 2016. Acid-modified montmorillonite for sorption of heavy
534 metals from automobile effluents. Beni-Suef Univ. J. Appl. Sci. 5, 1-12.

535 Alexiades, C.A.; Jackson, M. L., 1965. Quantitative determination of vermiculite in soils. Soil Sci.
536 Soc. Am. Proc. 29, 522-527.

537 Amer, M.; Khalili, F.; Awad, A., 2010. Adsorption of lead, zinc and cadmium ions on
538 polyphosphate-modified kaolinite clay. J. Env. Chem. Ecotoxicol. 2, 1-8.

539 Aziz, Z.; Bostick, B.C.; Zheng, Y.; Huq, M.R.; Rahman, M.M.; Ahmed, K.M.; Van Geen, A.,
540 2016. Evidence of decoupling between arsenic and phosphate in shallow groundwater of
541 Bangladesh and potential implications. Appl. Geochem. 1-11,
542 http://dx.doi.org/10.1016/j.apgeochem.2016.03.001.

543 Bhattacharyya, P.; Chatterjee, D.; Jacks, G., 1997. Occurrence of arsenic contaminated
544 groundwater in alluvial aquifers from delta plains, Eastern India: Options for safe drinking
545 water supply. Int. J. Water Res. Dev. 13, 79- 92.

546 Bidwell, J. I.; Jepson, W.B.; Toms, G.L., 1970. The interaction of kaolinite with poly-phosphate
547 and polyacrylate in aqueous solutions-some preliminary results. Clay Miner. 8, 445-459.

548 Boddu, V.M.; Abburi, K.; Talbott, J.L.; Smith, E.D.; Haasch, R., 2008. Removal of arsenic (III)
549 and arsenic (V) from aqueous medium using chitosan-coated biosorbent. Water Res. 42,
550 633-642.

551 Chowdhury, U.K.; Biswas, B.K.; Chowdhury, T.R.; Samanta, G.; Mandal, B.K.; Basu, G.K.;
552 Chanda, C.R.; Lodh, D.; Saha, K.C.; Mukherjee, S.C.; Roy, S.; Kabir, S.; Ouamruzzaman,
553 Q.; Chakraborti, D., 2000. Groundwater arsenic contamination in Bangladesh and West
554 Bengal, India. Env. Health. Persp. 108, 393-397.
555 Das, D.K.; Sur, P.; Das, K., 2008. Mobilisation of arsenic in soils and in rice (*Oryza sativa* L.)
556 plants affected by organic matter and zinc application in irrigation water contaminated with
557 arsenic. Plant Soil. Env. 54, 30–37.
558 Das, I.; Ghosh, K.; Das, D.K.; Sanyal, S.K., 2011. Studies on fractionation of Arsenic in soil in
559 relation to crop uptake. Soil. Sediment Contam. 20, 790-809.
560 Datta, S.C., 2002. Threshold levels of release and fixation of phosphorus: Their nature and method
561 of determination. Commun. Soil Sci. Plant Anal. 33, 213-227.
562 Doušová, B.; Fuitová, L.; Grygar, T.; Machovič, V.; Koloušek, D.; Herzogová, L.; Lhotka, M.,
563 2009. Modified aluminosilicates as low-cost sorbents of As(III) from anoxic groundwater.
564 J. Hazard. Mater. 165, 134-140.
565 El Miz, M.; Sahil, S.; Chraibi, I.; El Bachiri, A.; Fauconnier, M.L.; Tahani, A., 2014.
566 Characterization and adsorption of pillared bentonite. Open J. Phys. Chem. 4, 98-116.
567 Farmer, V. C., 1974. The layer silicates. In: Farmer, V. C (Eds.), The infrared spectra of minerals,
568 Mineralogical Society Monograph 4. London, pp. 331–363.
569 Fayiga, A.O.; Saha, U.K., 2016. Arsenic hyper accumulating fern: Implications for remediation of
570 arsenic contaminated soils. Geoderma. 284, 132-143.
571 Gebreyowhannes, Y. B., 2009. Effect of silica and pH on arsenic removal by iron-oxide coated
572 sand. M.Sc. Thesis, UNESCO-IHE Institute for Water Education, Delft, The Netherlands.

573 Ghosh, K.; Das, I.; Das, D.K.; Sanyal, S.K., 2012. Evaluation of humic and fulvic acid extracts of
574 compost, oilcake, and soils on complex formation with arsenic. Soil Res. 50, 239-248.
575 Giles, C. H.; McEvans, T. H.; Nakhwa, S. N.; Smith, D., 1960. Studies in adsorption. Part XI: a
576 system of classification of adsorption isotherms and its use in diagnosis of adsorption
577 mechanism and measurement of specific surface areas of solids. J. Chem. Soc. 4, 3973–
578 3993.
579 Goldberg, S., 2002. Competitive adsorption of Arsenate and Arsenite on oxides and clay minerals.
580 Soil Sci. Soc. Am. J. 66, 413-421.
581 Grygar, T.; Hradil, D.; Bezdicka, P.; Dousova, B.; Capek, L.; Schneeweiss, O., 2007. Fe(III)
582 modified montmorillonite and bentonite: Synthesis, chemical and UV-vis spectral
583 characterization, arsenic sorption, and catalysis of oxidative dehydrogenation of propane.
584 Clays Clay Miner. 55, 165-176.
585 Hassan, U.J.; Abdu, S.G., 2014. Structural analysis and surface morphology of kaolin. Sci. World
586 J. 9, 33-37.
587 Heilman, M.D.; Carter, D.L.; Gonzalez, C.L., 1965. The ethylene glycol monoethyl ether (EGME)
588 technique for determining soil surface area. Soil Sci. 100, 409-413.
589 Ioannou, A.; Dimirkou, A., 1997. Phosphate adsorption on hematite, kaolinite, and kaolinite–
590 hematite (k–h) systems as described by a constant capacitance model. J. Colloid Interface
591 Sci. 192, 119-128.
592 Jadhav, S.V.; Bringas, E.; Yadav, G.D.; Rathod, V.K.; Ortiz, I.; Marathe, K.V., 2015. Arsenic and
593 fluoride contaminated groundwaters: A review of current technologies for contaminants
594 removal. J. Environ. Manage. 162, 306-325.

595 Karamanis, D.T.; Aslanoglou, X.; Assimakopoulos, P.A.; Gangas, N.H.; Pakou, A.; Papayanakos,
596 N., 1997. An aluminium pillared montmorillonite with fast uptake of cesium and strontium
597 from aqueous system. Clays Clay Miner. 45, 709-717.
598 Khan, M.A.; Islam, M. R.; Panaullah, G.M.; Duxbury, J.M.; Jahiruddin, M.; Loeppert, H., 2009.
599 Fate of irrigation water arsenic in rice soils of Bangladesh. Plant Soil. 322, 263–277.
600 Kumararaja, P.; Manjaiah, K.M.; Datta, S.C.; Sarkar, B., 2017. Remediation of metal contaminated
601 soil by aluminium pillared bentonite: Synthesis, characterisation, equilibrium study and
602 plant growth experiment. Appl. Clay Sci. 137, 115-122.
603 Kumpiene, J.; Lagerkvist, A.; Maurice, C., 2008. Stabilization of As, Cr, Cu, Pb and Zn in soil
604 using amendments – A review. Waste Manage. 28, 215-225.
605 Lee, S.-H.; Kim, E.Y.; Park, H.; Yun, J.; Kim, J.-G., 2011. In situ stabilization of arsenic and
606 metal-contaminated agricultural soil using industrial by-products. Geoderma 161, 1-7.
607 Lenoble, V.; Bouras, O.; Deluchat, V.; Serpaud, B.; Bollinger, J., 2002. Arsenic adsorption onto
608 pillared clays and iron oxides. J. Colloid Interface Sci. 255, 52-58.
609 Li, Z.; Beachner, R.; Mcmanama, Z.; Hanlie, H., 2007. Sorption of arsenic by surfactant-modified
610 zeolite and kaolinite. Micropor. Mesopor. Mat. 105, 291-297.
611 Lim, J.E.; Sung, J.K.; Sarkar, B.; Wang, H.; Hashimoto, Y.; Tsang, D.C.W.; Ok, Y.S., 2016.
612 Impact of natural and calcined starfish (*Asterina pectinifera*) on the stabilization of Pb, Zn
613 and As in contaminated agricultural soil. Environ. Geochem. Health. 1-11,
614 doi:10.1007/s10653-016-9867-4.
615 Liu, J.; Zheng, B.S.; Aposhian, H.V.; Zhou, Y.S.; Chen, M.L.; Zhang, A.H.; Waalkes, M.P., 2002.
616 Chronic arsenic poisoning from burning high-arsenic-containing coal in Guizhou, China.
617 Environ. Health Perspect. 110, 119-122.

618 Lombi, E.; Hamon, R.E.; Wieshammer, G.; McLaughlin, M.J.; McGrath, S.P., 2004. Assessment
619 of the use of industrial by-products to remediate a copper- and arsenic-contaminated Soil.
620 J. Environ. Qual. 33, 902-910.
621 Ma, C.; Eggleton, R.A., 1999. Surface layer types of kaolinite: A high resolution transmission
622 electron microscope study. Clays Clay Miner. 47, 181-191.
623 Madejová, J.; Komadel, P., 2001. Baseline studies of the clay minerals society source clays:
624 Infrared methods. Clays Clay Miner. 49, 410-432.
625 Mandal, B.K.; Chowdhury, T.R.; Samanta, G.; Basu, G.K.; Chowdhury, P.P.; Chanda, C.R.; Lodh,
626 D.; Naran, N.K.; Dhara, R.K.; Tamili, D.K.; Das, D.; Saha, K.C.; Chakraborti, D., 1996.
627 Arsenic in groundwater in seven districts of West Bengal, India – the biggest arsenic
628 calamity in the world. Curr. Sci. 70, 976- 986.
629 Mandal, A.; Purakayastha, T.J.; Patra, A.K.; Sanyal, S.K., 2012. Phytoremediation of arsenic
630 contaminated soil by *Pteris vittata* L. II. Effect on arsenic uptake and rice yield. Int. J.
631 Phytoremediation. 14, 621-628.
632 Mandal, A.; Purakayastha, T.J.; Patra, A.K.; Sarkar, B., 2017. Arsenic phytoextraction by *Pteris*
633 *vittata* improves microbial properties in contaminated soil under various phosphate
634 fertilizations. Appl. Geochem. doi: 10.1016/j.apgeochem.2017.04.008.
635 Manna, B. R.; Dey, S.; Debnath, S.; Ghosh, U. C., 2003. Removal of arsenic from groundwater
636 using crystalline hydrous ferric oxide (CHFO). Water Qual. Res. J. Can. 38, 193–210.
637 Manning, B. A.; Goldberg, S., 1996. Modeling arsenate competitive adsorption on kaolinite,
638 montmorillonite and illite. Clays Clay Miner. 44, 609-623.
639 Marschner, H., 1995. *Mineral Nutrition of Higher Plants*. Academic Press, New York.

640 Miretzky, P.; Cirelli, A.F., 2010. Remediation of arsenic-contaminated soils by iron amendments:
641 A review. Crit. Rev. Env. Sci. Technol. 40, 93-115.
642 Mohan, D.; Pittman Jr, C.U., 2007. Arsenic removal from water/wastewater using adsorbents- A
643 critical review. J. Hazard. Mater. 142, 1-53.
644 Mohapatra, D.; Mishra, D.; Roy Chaudhury, G.; Das, R. P., 2007. Arsenic adsorption mechanism
645 on clay minerals and its dependence on temperature. Korean J. Chem. Eng. 24, 426-430.
646 Mukhopadhyay, D.; Mani, P.K.; Sanyal, S.K., 2002. Effect of phosphorus, arsenic and farmyard
647 manure on arsenic availability in some soils of West Bengal. J. Ind. Soc. Soil Sci. 50, 56-
648 61.
649 Na, P.; Jia, X.; Yuan, B.; Li, Y.; Na, J.; Chen, Y.; Wang, L., 2010. Arsenic adsorption on Ti-
650 pillared montmorillonite. J. Chem. Technol. Biot. 85, 708-714.
651 Niazi, N.K.; Bashir, S.; Bibi, I.; Murtaza, B.; Shahid, M.; Javed, M.T.; Shakoor, M.B.; Saqib, Z.A.;
652 Nawaz, M.F.; Aslam, Z.; Wang, H.; Murtaza, G., 2016. Phytoremediation of arsenic-
653 contaminated soils Using Arsenic hyper accumulating ferns. In: Ansari, A.A.; Gill, S.S.;
654 Gill, R.; Lanza, G.R.; Newman, L. (Eds.). Phytoremediation: Management of
655 Environmental Contaminants, Volume 3. Springer International Publishing, Cham, pp. 521-
656 545.
657 Ng, J.C.; Wang, J.; Shraim, A., 2003. A global health problem caused by arsenic from natural
658 sources. Chemosphere. 52, 1353-1359.
659 Perelomov, L.; Sarkar, B.; Rahman, M.M.; Goryacheva, A.; Naidu, R., 2016. Uptake of lead by
660 Na-exchanged and Al-pillared bentonite in the presence of organic acids with different
661 functional groups. Appl. Clay Sci. 119, Part 2, 417-423.
662 Pontius, F.W., 1994. Crafting a new arsenic rule. J. Am. Water Works Assoc. 86, 6.

663 Ramesh, A.; Hasegawa, H.; Maki, T.; Ueda, K., 2007. Adsorption of inorganic and organic arsenic
664 from aqueous solutions by polymeric Al/Fe modified montmorillonite. Sep. Purif Technol.
665 56, 90-100.
666 Rivaz-Perez, I.M.; Paradelo-Nunez, R.; Novoa-Munoz, J.C.; Arias-Estevez, M.; Fernandez-
667 Sanjurjo, M.J.; Álvarez-Rodríguez, E.; Núñez-Delgado, A., 2015. As(V) and P competitive
668 sorption on soils, by-products and waste materials. Int. J. Environ. Res. Public Health. 12,
669 15706-15715.
670 Rusmin, R.; Sarkar, B.; Biswas, B.; Churchman, J.; Liu, Y.; Naidu, R., 2016. Structural,
671 electrokinetic and surface properties of activated palygorskite for environmental
672 application. Appl. Clay Sci. 134, Part 2, 95-102.
673 Sanyal, S.K., 1999. Chemodynamics of geogenic contaminants in the soil environment-Arsenic.
674 In: Proceedings of the Second International. Conference on Contaminants in the Soil
675 Environment in the Australasia-Pacific Region, New Delhi, December 12-17, 1999.
676 Extended Abstracts, pp. 389-390. Indian Network for Soil Contamination Research, New
677 Delhi, India and Soil Contamination Research in Asia and the Pacific, Adelaide, Australia.
678 Sanyal, S.K.; Nasar, S.K.T., 2002. Arsenic contamination of groundwater in West Bengal (India):
679 build-up in soil-crop system. In 'Analysis and practice in water resources engineering for
680 disaster mitigation'. Volume 1. Indian Association of Hydrologists. pp. 216–222. (New Age
681 International Publishers: New Delhi).
682 Sarkar, A.; Paul, B., 2016. The global menace of arsenic and its conventional remediation - A
683 critical review. Chemosphere. 158, 37-49.

684 Sarkar, B.; Naidu, R.; Megharaj, M., 2013. Simultaneous adsorption of tri- and hexavalent
685 chromium by organoclay mixtures. Water Air Soil Pollut. 224, 1704, doi: 10.1007/s11270-
686 013-1704-0.
687 Sarkar, B.; Naidu, R.; Rahman, M.M.; Megharaj, M.; Xi, Y., 2012. Organoclays reduce arsenic
688 bioavailability and bio accessibility in contaminated soils. J. Soils Sediments. 12, 704-712.
689 Seki, Y.; Yurdakoc, K., 2007. Identification and characterization of Fe-rich smectites in the C¸
690 amlıca Region of western Turkey. Clay Miner. 42, 153-160.
691 Shakoor, M.B.; Niazi, N.K.; Bibi, I.; Murtaza, G.; Kunhikrishnan, A.; Seshadri, B.; Shahid, M.;
692 Ali, S.; Bolan, N.S.; Ok, Y.S.; Abid, M.; Ali, F., 2016. Remediation of arsenic-contaminated
693 water using agricultural wastes as biosorbents. Crit. Rev. Env. Sci. Technol. 46, 467-499.
694 Sharma, A.K.; Tjell, J.C.; Sloth, J.J.; Holm, P.E., 2014. Review of arsenic contamination, exposure
695 through water and food and low cost mitigation options for rural areas. Appl Geochem. 41,
696 11-33.
697 Shevade, S.; Ford, R.G., 2004. Use of synthetic zeolites for arsenate removal from pollutant water.
698 Water Res. 38, 3197-3204.
699 Sparks, D. L., 1989. *Kinetics of soil chemical processes*. Academic Press, Inc., New York.
700 Stucki, J.W.; Lee, K.; Zhang, L.; Larson, R.A., 2002. Effects of iron oxidation state on the surface
701 and structural properties of smectites. Pure Appl. Chem. 74, 2145-2158.
702 Suda, A.; Makino, T., 2016. Effect of organic amendments on arsenic solubilization in soils during
703 long-term flooded incubation. Int. J. Env. Sci. Technol. 13, 2375-2382.
704 Sun, Y.; Sun, G.; Xu, Y.; Wang, L.; Liang, X.; Lin, D., 2013. Assessment of sepiolite for
705 immobilization of cadmium-contaminated soils. Geoderma. 193–194, 149-155.

706 Te, B.; Wichitsathian, B.; Yossapol, C., 2015 Modification of natural common clays as low cost
707 adsorbents for arsenate adsorption. Int. J. Env. Sci. Dev. 6, 799-804.
708 Thirunavukkarasu, O.S.; Viraraghavan, T.; Subramanian, K.S., 2001. Removal of arsenic in
709 drinking water by iron oxide-coated sand and ferrihydrite - batch studies. Wat. Qual. Res.
710 J. Can. 36, 55–70.
711 Thomas, D. J.; Styblo, M.; Lin, S., 2001. The cellular metabolism and systemic toxicity of arsenic.
712 Toxicol. Appl. Pharm. 176, 127-144.
713 Treybal, R.E., 1980. *Mass Transfer Operations*, third ed., McGraw-Hill, New York.
714 Unuaboanh, E.I.; Adebowale, K.O; Olu-owalabi, B.I., 2007. Kinetic and thermodynamic studies
715 for adsorption of lead (II) ions onto phosphate- modified kaolinite clay. J. Hazard. Mater.
716 144, 386-395.
717 Unuaboanh, E.I.; Olu-owalabi, B.I.; Adebowale, K.O.; Yang, L.Z., 2008. Removal of lead and
718 cadmium Ions from aqueous solution by polyvinyl alcohol-modified kaolinite clay: A novel
719 nano-clay adsorbent. Adsorpt. Sci. Technol. 26, 383-405.
720 Violante, A.; Pinga, M., 2002. Competitive sorption of srsenate and phosphate on different
721 clay minerals and soils. Soil Sci. Soc. Am. J. 66, 1788-1796.
722 Vithanage, M.; Herath, I.; Joseph, S.; Bundschuh, J.; Bolan, N.; Ok, Y.S.; Kirkham, M.B.;
723 Rinklebe, J., 2017. Interaction of arsenic with biochar in soil and water: A critical review.
724 Carbon. 113, 219-230.
725 Wang, P.; Liu, Y.; Menzies, N.W.; Wehr, J.B.; de Jonge, M.D.; Howard, D.L.; Kopittke, P.M.;
726 Huang, L., 2016. Ferric minerals and organic matter change arsenic speciation in copper
727 mine tailings. Environ. Pollut. 218, 835-843.

728 Xu, H.; Allard, B.; Grimvall, A., 1988. Influence of pH and organic substance on the adsorption
729 of As(V) on geologic materials. Water Air Soil Pollut. 40, 293-305.
730 Zeng, L., 2004. Arsenic adsorption from aqueous solutions on an Fe(III)-Si binary oxide adsorbent.
731 Water Qual. Res. J. Can. 39, 267-275.
732 Zhang, Y.; Song, S.; Zhang, M., 2008. Preparation and characterization of titanium - pillared
733 montmorillonite. Surf. Rev. Lett. 15, 329-336.
734

Tables

Table 1: Physico-chemical properties of arsenic contaminated soil (Mitrapur, West Bengal, India)

Properties	Values
Clay (%)	26.5
Sand (%)	23.2
Silt (%)	50.3
Textural Class	Silty clay loam
pH (1:2.5)	6.49
EC (dS m^{-1})	0.26
Organic carbon (g kg^{-1})	4.50
Amorphous Fe (%)	0.29
Total Fe (%)	1.31
Total As (mg kg^{-1})	14.1
Olsen extractable As (mg kg^{-1})	3.6
CEC [cmol (p^+) kg^{-1}]	24.7

Table 2: Characteristics of unmodified and modified clay minerals

Clay minerals	pH (1:2.5)	Specific surface area (m^2 g^{-1})	Cation exchange capacity [cmol (p^+) kg^{-1}]	d(001) (Å)
Unmodified smectite	8.20	202.69	118.50	14.24
Fe-exchanged smectite	3.93	485.62	115.75	16.35
Ti-pillared smectite	5.95	437.06	105.75	16.97
Unmodified kaolinite	6.75	18.40	22.25	7.25
Phosphate-bound kaolinite	6.50	89.08	40.50	7.13

Table 3: Estimated kinetic model parameters for arsenic adsorption on unmodified and modified clay minerals in aqueous medium

Models	Parameter	Ti-pillared smectite	Fe-exchanged smectite	Unmodified smectite	Phosphate-bound kaolinite	Unmodified kaolinite
Power function	a	398.66	475.78	408.56	397.2	435.18
	b	0.039	0.038	0.051	0.047	0.026
	R^2	0.92	0.95	0.97	0.98	0.96
Simple Elovich	a	392.88	469.12	398.2	389.43	432.76
	b	18.31	21.04	25.56	22.35	12.48
	R^2	0.92	0.94	0.97	0.98	0.96

The initial As addition was 50 μg As mL^{-1}, solid: solution = 1: 20, and pH maintained at 6.2

Table 4: Average partition coefficient (K_d) and adsorption efficiency of arsenic for different unmodified and modified clay minerals in aqueous and soil systems

Clays	K_d (mL g^{-1}) in aqueous system	K_d (mL g^{-1}) in soil system	Adsorption efficiency in aqueous system (%)	Adsorption efficiency in soil system (%)
Unmodified smectite	67.30	47.15	48.56	53.80
Fe-exchanged smectite	121.89	100.13	73.64	72.08
Ti-pillared smectite	175.77	85.45	78.82	68.58
Unmodified kaolinite	85.20	54.48	66.07	58.36
Phosphate-bound kaolinite	109.46	70.70	79.05	66.90

Table 5: Freundlich isotherm model constants for arsenic adsorption on different unmodified and modified clay minerals in aqueous and soil systems

Adsorption system	Parameters	Ti-pillared smectite	Fe-exchanged smectite	Unmodified smectite	Phosphate-bound kaolinite	Unmodified kaolinite
Aqueous	K (μg/g $(mL/\mu g)^{1/n}$)	156.54	127.63	66.03	124.43	93.82
	1/n	0.46	0.46	0.39	0.62	0.50
	R^2	0.91	0.93	0.48	0.92	0.65
Soil	K (μg/g $(mL/\mu g)^{1/n}$)	104.19	115.63	65.54	95.05	68.65
	1/n	0.48	0.49	0.46	0.49	0.53
	R^2	0.86	0.85	0.63	0.85	0.66

Figures

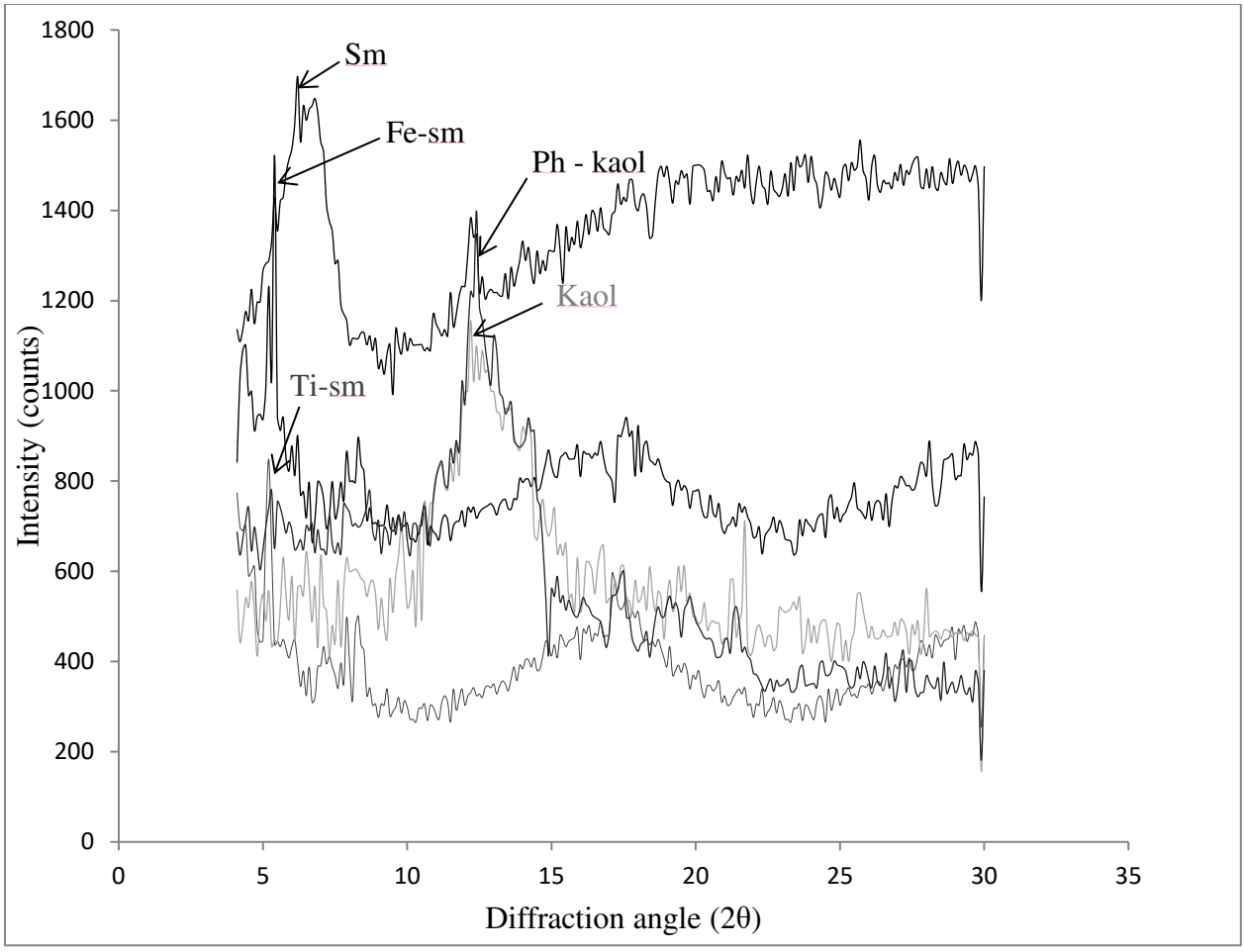

Fig. 1 X-ray diffraction patterns of unmodified smectite (Sm), Ti-pillared smectite (Ti-sm), Fe-exchanged smectite (Fe-sm), unmodified kaolinite (Kaol) and phosphate-bound kaolinite (Ph-kaol)

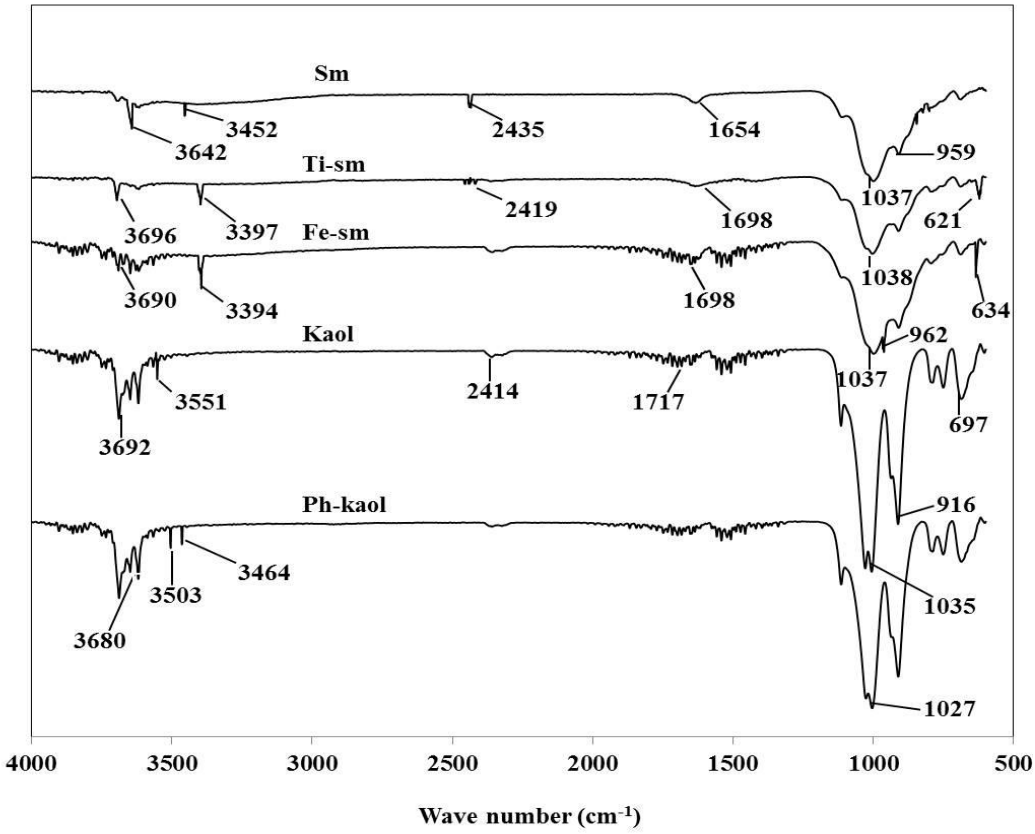

Fig. 2 FT-IR spectra of unmodified smectite (Sm), Ti-pillared smectite (Ti-sm), Fe-exchanged smectite (Fe-sm), unmodified kaolinite (Kaol) and phosphate-bound kaolinite (Ph-kaol)

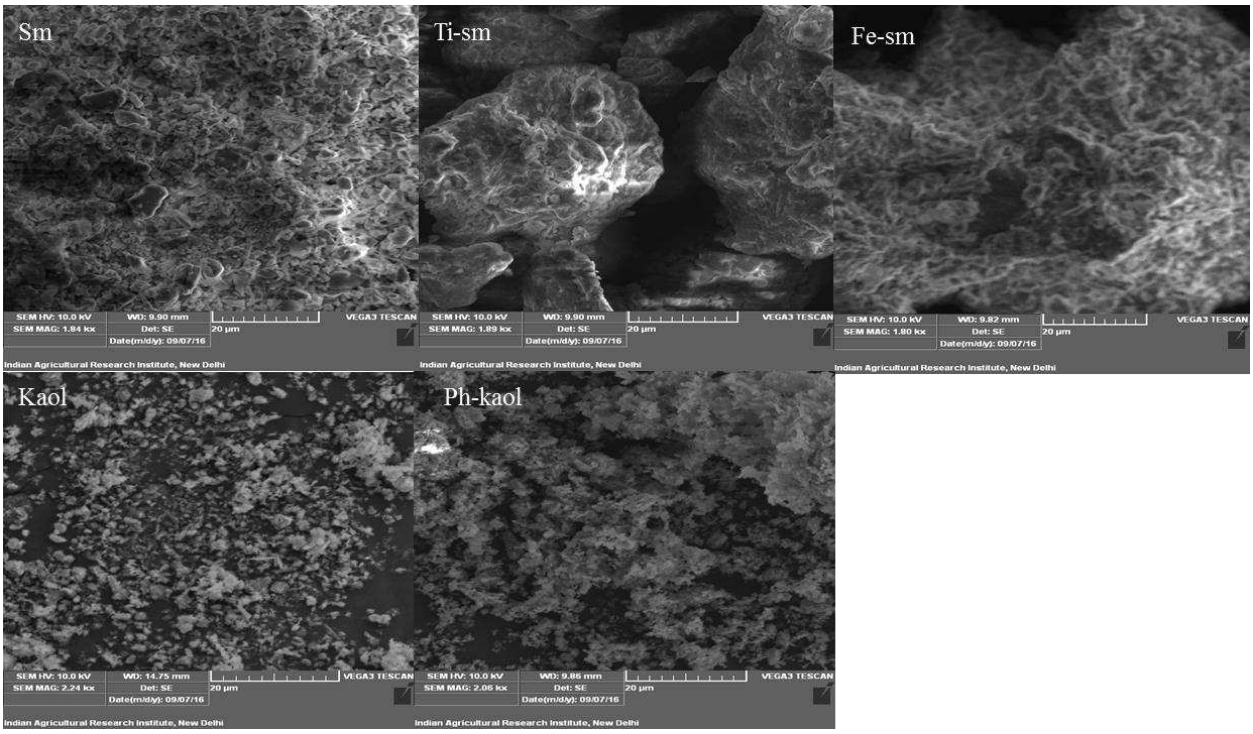

Fig. 3 SEM images of unmodified smectite (Sm), Ti-pillared smectite (Ti-sm), Fe-exchanged smectite (Fe-sm), unmodified kaolinite (Kaol) and phosphate-bound kaolinite (Ph-kaol)

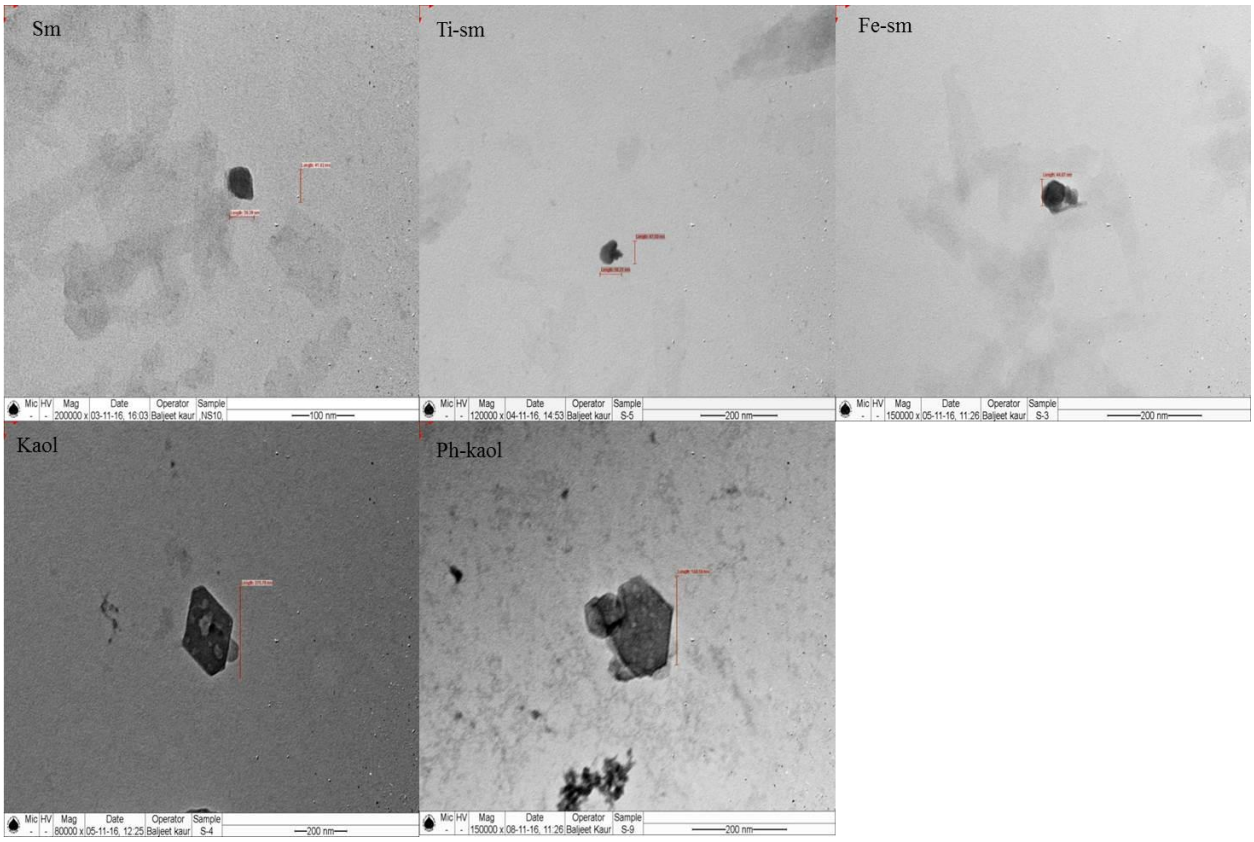

Fig. 4 TEM images of unmodified smectite (Sm), Ti-pillared smectite (Ti-sm), Fe-exchanged smectite (Fe-sm), unmodified kaolinite (Kaol) and phosphate-bound kaolinite (Ph-kaol)

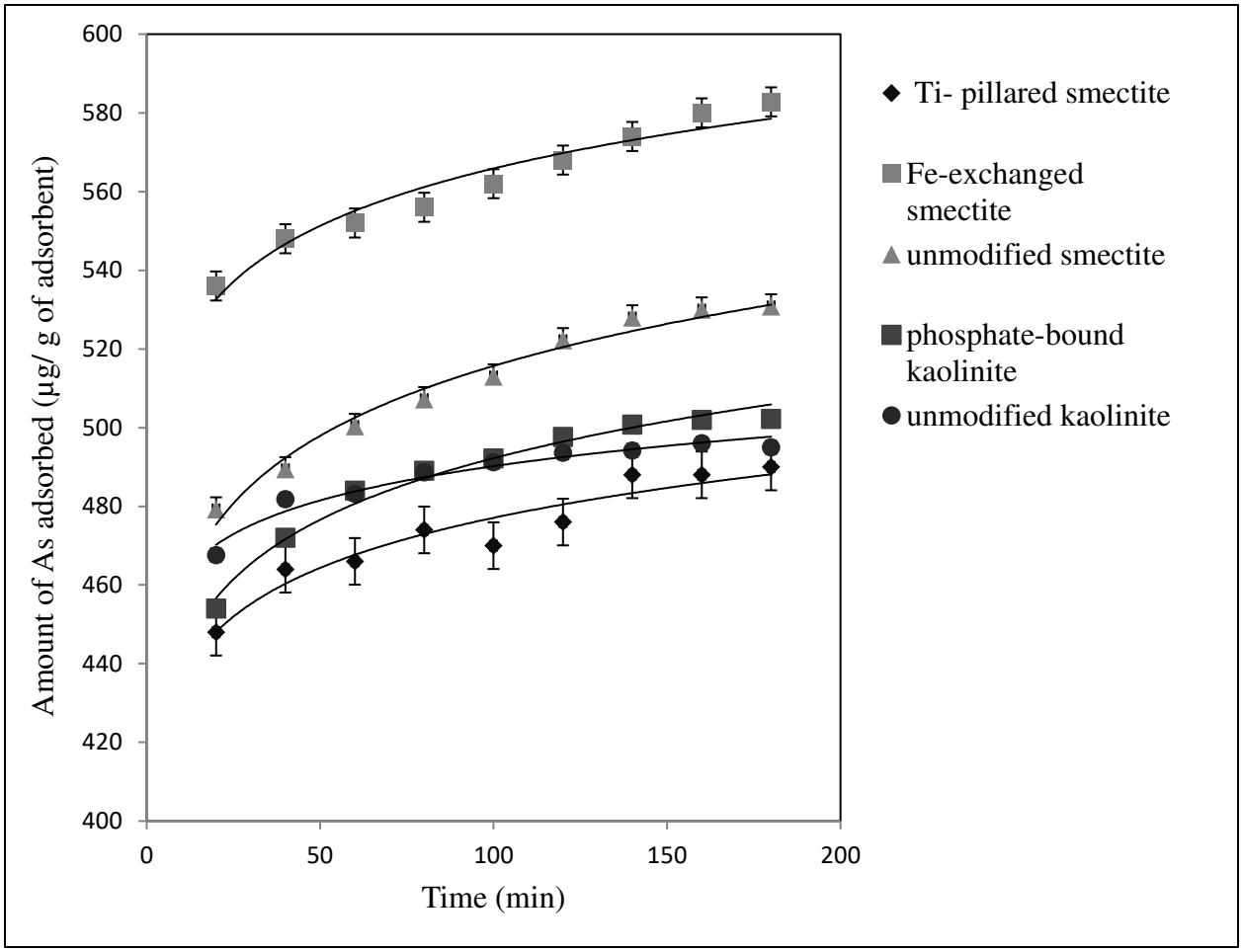

Fig. 5 Kinetics of arsenic adsorption onto unmodified, Ti-pillared, Fe-exchanged smectites, and unmodified and phosphate-bound kaolinites in aqueous system (the fitting curves represent the power function equation).

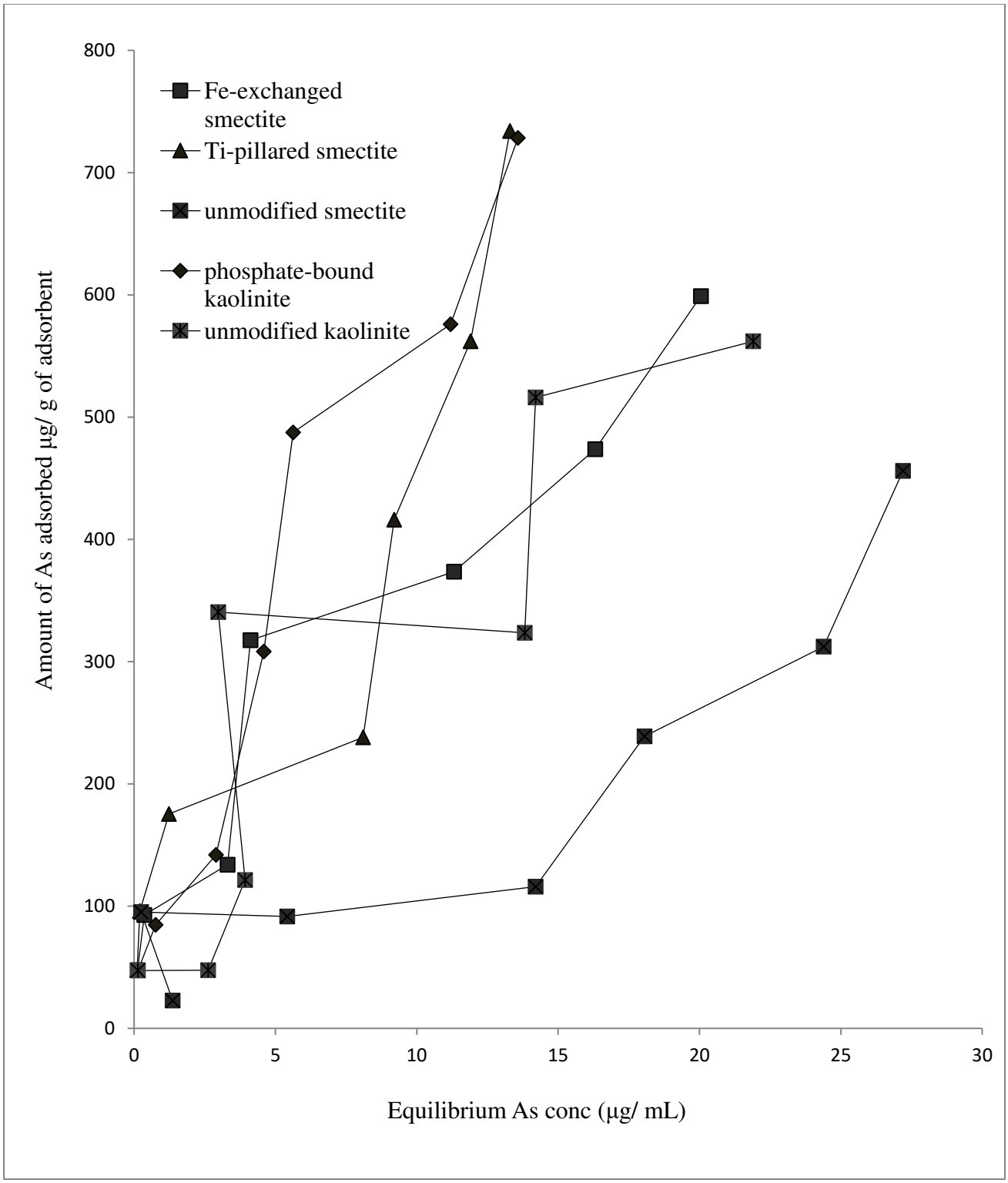

Fig. 6 Arsenic adsorption isotherm onto unmodified, Ti-pillared and Fe-exchanged smectites, and unmodified and phosphate-bound kaolinites in aqueous system (the curves were best fitted in Freundlich adsorption isotherm).

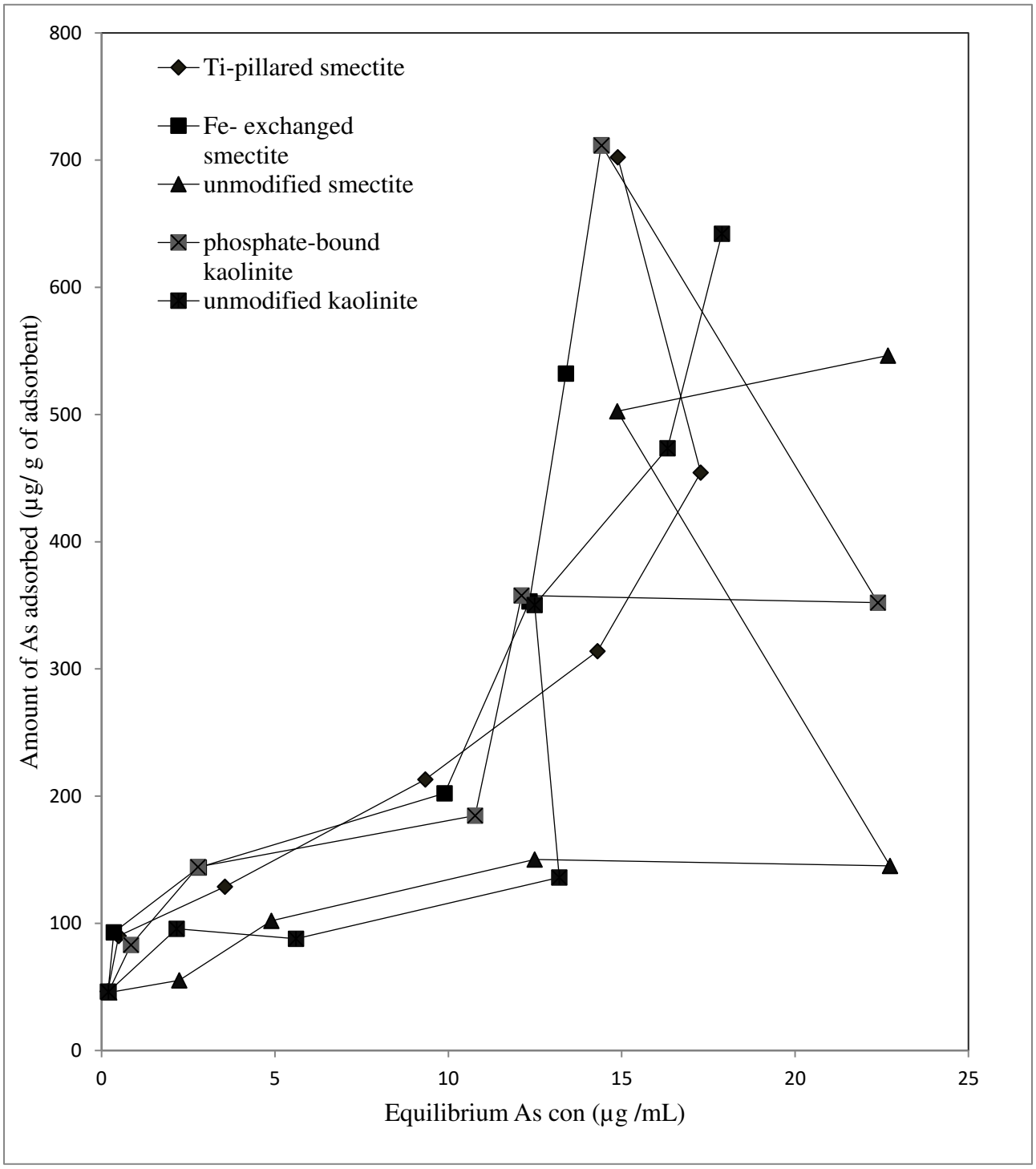

Fig. 7 Arsenic adsorption isotherm onto unmodified, Ti-pillared and Fe-exchanged smectites, and unmodified and phosphate-bound kaolinites in soil system (the curves were best fitted in Freundlich adsorption isotherm).